X Congreso Regional Latinoamericano IRPA de Protección y Seguridad Radiológica
"Radioprotección: Nuevos Desafíos para un Mundo en Evolución"
Buenos Aires, 12 al 17 de abril, 2015
SOCIEDAD ARGENTINA DE RADIOPROTECCIÓN

ESTIMATION OF ORGAN DOSES OF PATIENT UNDERGOING HEPATIC CHEMOEMBOLIZATION PROCEDURES

Jaramillo, G.W.[1], Kramer, R.[1], Khoury, H.J.[1], Barros, V.S.M.[1] and Andrade, G.[2]

[1] Department of Nuclear Energy, Federal University of Pernambuco, Recife, Brazil
[2] Angiorad, Recife, Brazil

ABSTRACT

The aim of this study is to evaluate the organ doses of patients undergoing hepatic chemoembolization procedures performed in two hospitals in the city of Recife-Brazil. Forty eight patients undergoing fifty hepatic chemoembolization procedures were investigated. For the 20 cases with PA projection only, organ and tissue absorbed doses as well as radiation risks were calculated. For this purpose organs and tissues dose to KAP conversion coefficients were calculated using the mesh-based phantom series FASH and MASH coupled to the EGSnrc Monte Carlo code. Clinical, dosimetric and irradiations parameters were registered for all patients. The maximum organ doses found were 1.72 Gy, 0.65Gy, 0.56 Gy and 0.33 Gy for skin, kidneys, adrenals and liver, respectively.

1. INTRODUCTION

Hepatic chemoembolization interventional procedures have been recognized for delivering high skin doses to patients. In many cases patients require repeated chemoembolizations to be performed for the same lesion. Re-irradiation of the skin and organs may significantly increase the probability of radiation effects. Several studies have reported the maximum skin dose and the air-kerma area product (KAP) for the assessment of patient radiation exposure for this procedure [1, 2, 3]. However, few estimates of organ and tissue absorbed doses have been done so far.

In patient dosimetry for interventional radiology, it is common to use specific conversion coefficients (CCs) for estimating the organ and tissue absorbed dose to patients. The CCs are defined as the ratio between the absorbed dose to a specified organ or tissue and a normalization quantity, like the air kerma–area product KAP, for example [4]. CCs are usually determined by Monte Carlo calculations.

The ICRP recommends the use of reference computational phantoms for the adult reference male and female for the calculation of organs and tissue CCs [5]. The main problem when using a CC is the anatomical correspondence between patient and phantom. In a study in interventional procedures, Johnson et al [6] showed that if the patient size is neglected when choosing a CC, organ and tissue absorbed doses will be underestimated for an underweight patient and will be overestimated for an overweight patient, with errors as large as 113% for certain projections.

[1] E-mail del Autor. wjaramig@gmail.com

Therefore, the use of phantoms with different body masses and/or heights for the Monte Carlo calculations would certainly improve the organ and tissue absorbed dose assessments for populations such as patients [7].

2. MATERIALS AND METHODS

This study investigated 50 hepatic chemoembolization procedures for 48 patients diagnosed with hepatocellular carcinoma which have been treated in two hospitals in the city of Recife-Brazil. Table 1 summarizes the anthropometric data of the patients per hospital and gender.

Table 1. Anthropometric data of the patients

Hospital Equipment	Patient Gender/ Number	Age (y) Mean Min-Max	Mass (kg) Mean Min-Max	Height (cm) Mean Min-Max
A Siemens	F/10	56,86 (25-81)	59,40 (49-68)	159,25 (155-165)
	M/18	65,27 (35-89)	63,59 (49-81)	164,82 (155-178)
B Philips	F/10	65,57 (51-85)	73,40 (60-100)	158,80 (152-162)
	M/10	67,60 (53-78)	89 (80-101)	170,20 (165-174)

The examinations were carried out with a Siemens Artis zee (hospital A) and a Philips Allura FD 20 equipment (hospital B), both equipped with flat panel technology. The projections used by the physicians were PA for 20 cases, PA and 26° RAO/12° CRA for 20 cases and PA and 23° RAO/12° CAU for 10 cases. The dose protocols used in the procedures were adjusted by the technicians of the room. In all procedures, pulsed fluoroscopy and a low rate of image acquisition was used.

For each procedure the following patient exposure data were recorded: tube potential, current, pulse length, fluoroscopy time, number of images, field-of-view (FOV), source-to-detector distance (SDD) and the KAP. The KAP meters of both equipment were calibrated using the under couch installation methodology described in IAEA code of practice [8].

For the 20 cases with PA projections, organ and tissue absorbed doses as well as radiation risks were calculated with anthropometric supine adult human phantoms. Applying to the standing anthropometric adult human MASH/FASH phantoms (Cassola et al 2011) the methodology developed by Cassola et al 2010 [9], 9 supine phantoms for each gender with three different body masses and three different heights have been designed. These phantoms are used by the online dose calculator CALDose_X [10]. Figures 1 and 2 show the male and female anthropometric adult phantoms, respectively, for 3 different body masses and 3 different heights, with the masses and heights shown in table 2.

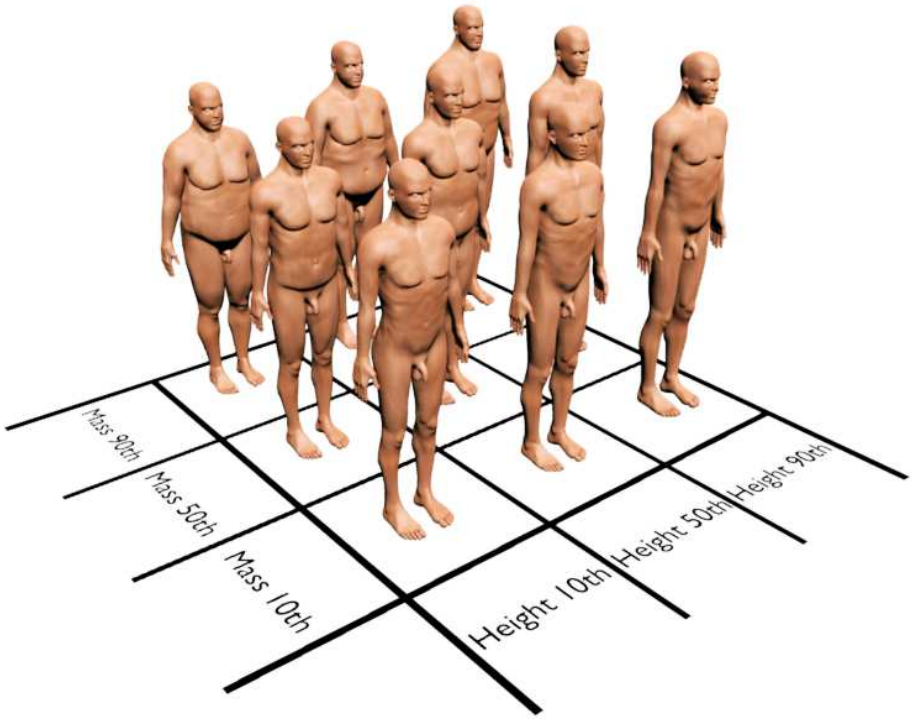

Figure 1. Male adult anthropometric MASH phantoms

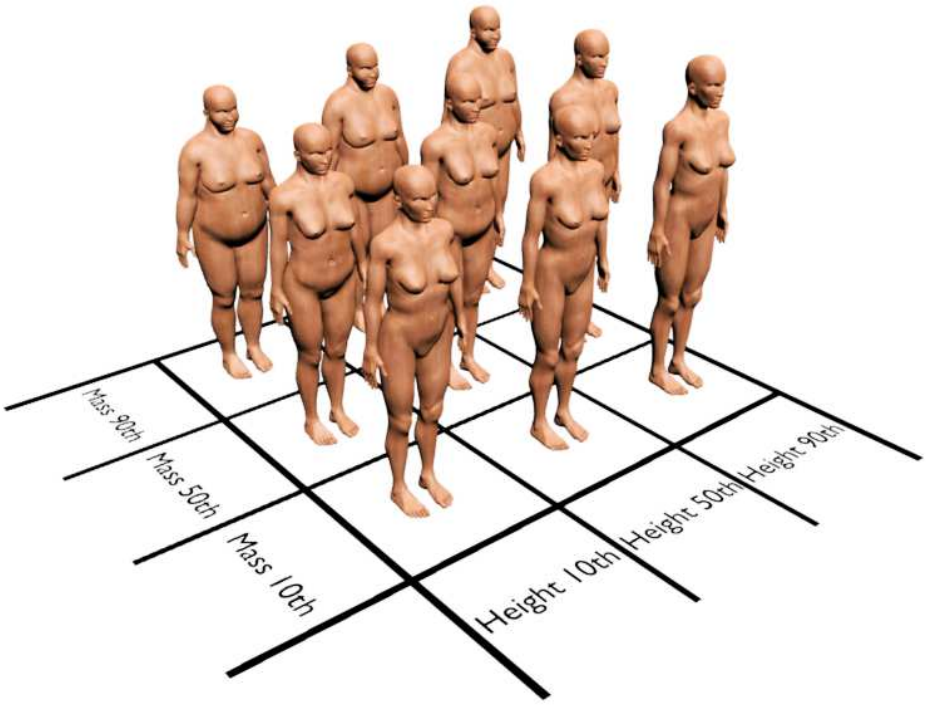

Figure 2. Female adult anthropometric FASH phantoms

Table 2. Body masses and heights for the anthropometric MASH and FASH phantoms

	FEMALE ADULT			MALE ADULT		
Percentil	MASS 10th	MASS 50th	MASS 90th	MASS 10th	MASS 50th	MASS 90th
HEIGHT 10th	48.6 kg 155.5 cm	58.5 kg 155.5 cm	76.7 kg 155.5 cm	59.3 kg 167.3 cm	71.1 kg 167.3 cm	88.2 kg 167.3 cm
HEIGHT 50th	54 kg 163.8 cm	65 kg 163.8 cm	85 kg 163.8 cm	66 kg 176.4 cm	79 kg 176.4 cm	98 kg 176.4 cm
HEIGHT 90th	59.6 kg 172.2 cm	71.8 kg 172.2 cm	94 kg 172.2 cm	73.0 kg 185.6 cm	87.5 kg 185.6 cm	108.5 kg 185.6 cm

Using the anthropometric MASH and FASH phantoms shown in figures 1 and 2, CCs between organ and tissue absorbed doses and the KAP were calculated with the EGSnrc Monte Carlo code [11], for the 20 cases of PA projection, taking into account body masses and heights of the patients as closely as possible to the phantom data shown in table 2.

Table 3 shows the tube potentials and filtration of the equipments used during the procedures in hospitals A and B. For the Monte Carlo simulations, X-ray spectra have been generated using these data and the IPEM 78 catalogue of spectra [12]. For all simulations a field size at the detector input of 35cm x 35cm and a focus- to patient distance of 70 cm were used.

Table 3. Beam qualities used in the Monte Carlo simulations

Hospital	kVp	Filtration	HVL (mm Al)
A	70	2.5 mm Al + 0.3 mm Cu	5,487
	80	2.5 mm Al + 0.3 mm Cu	6,307
B	90	3,5 mm Al + 0.4 mm Cu	7,78
	100	3,5 mm Al + 0.4mm Cu	8,42
	110	3,5 mm Al + 0.4 mm Cu	8,97

3. RESULTS AND DISCUSSION

In table 4, irradiation and patient dose parameters used in each hospital for male and female patients submitted to hepatic chemoembolization procedure are summarized. KAP values are significantly higher in hospital B, which will be explained later based on the data shown in tables 6 and 7.

Table 4. Mean values of irradiation and dose parameters per hospital and gender

Hospital	Patient gender	Irradiation parameters			Patient dosimetric parameters		
		Potential (kV)	Current (mA)	Pulse length (ms)	No of images	Fluoroscopy time (min)	KAP ($Gy*cm^2$)
A	F	66,73	147,44	12,70	205,63	20,13	136,52
	M	67,40	151,55	12,35	307,18	22,75	297,02
B	F	97,48	15,47	***	220,43	16,30	396,13
	M	100,69	15,87	***	255,20	15,96	513,76

***** unreported data**

Multiplication of the CCs with the measured KAP values of tables 6 and 7 gives the absolute organ and tissue absorbed doses per male and female patients in both hospitals shown in figures 3 and 4, respectively.

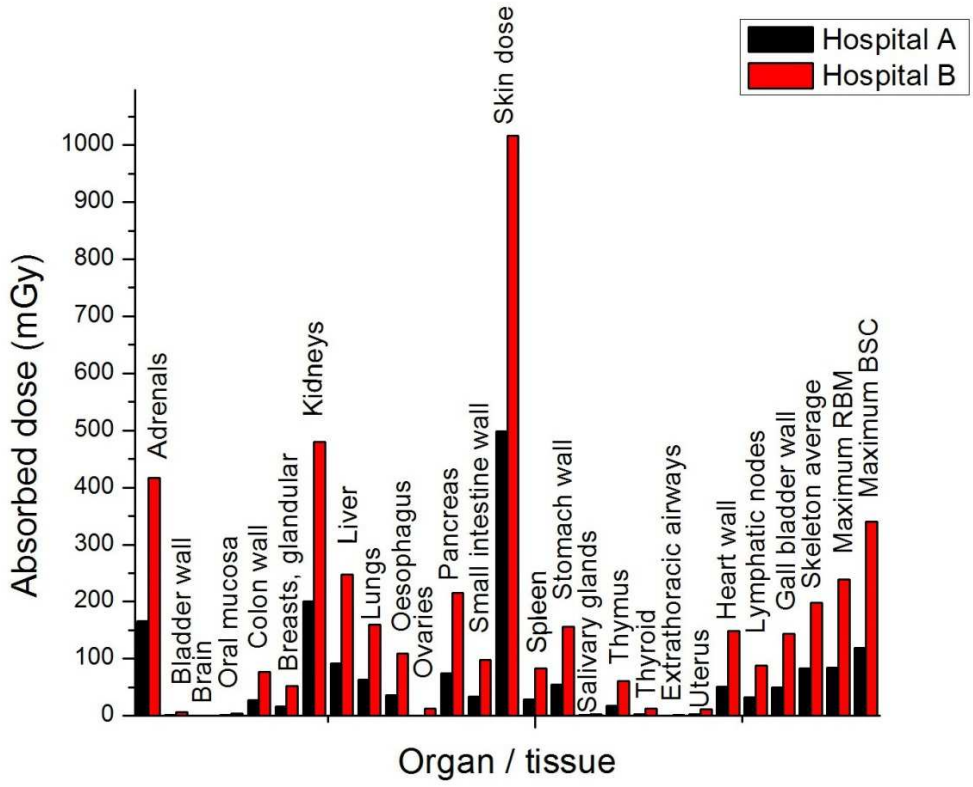

Figure 3. Mean female organ absorbed dose for PA projection

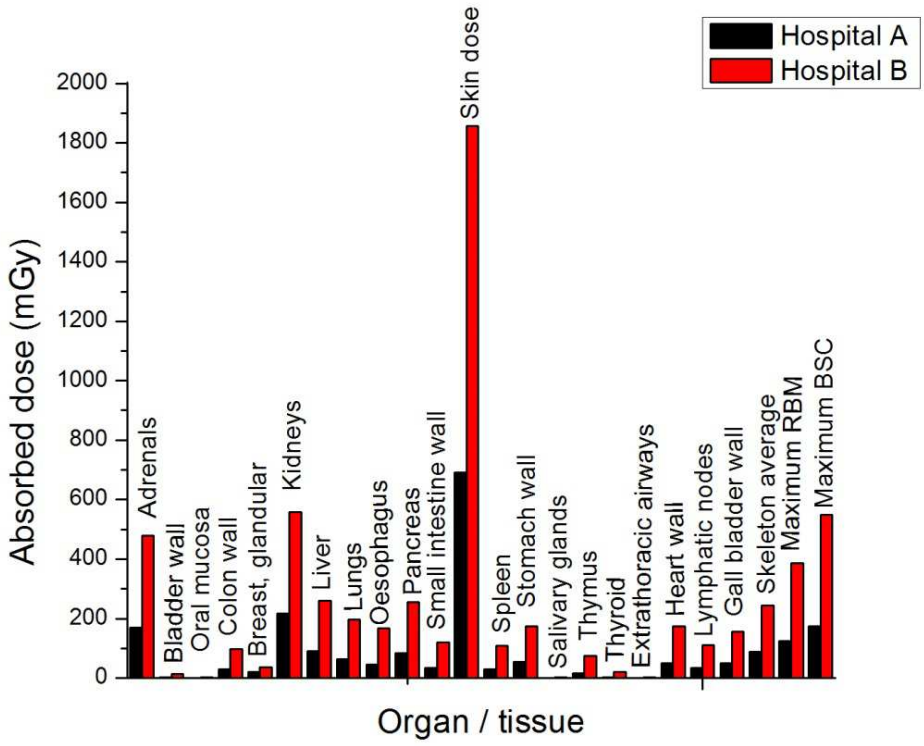

Figure 4. Mean male organ absorbed dose for PA projection

Organs or tissues showing the highest doses are the skin, kidneys, adrenals, liver, pancreas, and the skeletal tissues red bone marrow (RBM) and the bone surface cells (BSC). Table 5 shows the mean absorbed doses (AvDos) for these organs and tissues, together with the standard deviation (sd) and the range per hospital and gender. The skin absorbed dose was calculated in a 7.2 cm square of skin around the central axis of the beam at the entrance side, while RBM and BSC absorbed doses are the maximum absorbed dose found in a bone in the irradiated volume of the body.

Comparison with data from Hidajat et al [16] and Dauer et al [17] in table 5 show reasonable agreement with data from this study. One reason of this could be the agreement in the body mass of the patients between studies. For example the median body mass of patients in the Dauer's study was 79 kg that is comparable with the median body mass of patients for hospital B (82 kg) in this study.

Table 5. Absorbed doses (Gy) for the organs/tissues with the highest values for hospital A and B as a function of gender for PA projection

	Skin	Kidneys	BSC	Adrenals	RBM	Liver	Pancreas
Hospital A (12 subjects)							
AvDos±sd	0.62±0.54	0.20±0.14	0.16±0.11	0.16±0.10	0.11±0.08	0.09±0.05	0.08±0.05
Range	0.18-2.22	0.07-0.60	0.06-0.49	0.06-0.46	0.04-0.35	0.03-0.22	0.03-0.23
Hidajat et al		0.20±0.14		0.16±0.11		0.08±0.05	
9 male subjects							
AvDos±sd	0.72±0.60	0.22±0.15	0.18±0.12	0.17±0.11	0.13±0.1	0.09±0.05	0.09±0.06
Range	0.18-2.22	0.07-0.59	0.06-0.48	0.06-0.46	0.04-0.35	0.03-0.22	0.03-0.23
3 female subjects							
AvDos±sd	0.34±0.14	0.14±0.04	0.08±0.02	0.12±0.04	0.06±0.02	0.06±0.02	0.05±0.02
Range	0.21-0.48	0.10-0.19	0.06-0.11	0.08-0.16	0.05-0.08	0.05-0.09	0.04-0.07
Hospital B (8 subjects)							
AvDos±sd	1.66±0.63	0.58±0.21	0.50±0.18	0.50±0.19	0.35±0.13	0.29±0.11	0.27±0.10
Range	0.53-2.44	0.27-0.85	0.21-0.78	0.24-0.76	0.15-0.55	0.15-0.44	0.13-0.39
Dauer et al		0.54±0.35		0.50±0.31		0.19±0.12	0.14±0.09
4 male subjects							
AvDos±sd	1.72±0.50	0.51±0.17	0.51±0.18	0.44±0.16	0.36±0.13	0.24±0.08	0.24±0.08
Range	1.30-2.43	0.38-0.76	0.40-0.78	0.33-0.68	0.28-0.55	0.18-0.37	0.18-0.36
Dauer et al		0.59±0.32		0.54±0.27		0.20±0.10	0.15±0.08
4 female subjects							
AvDos±sd	1.60±0.81	0.65±0.26	0.49±0.20	0.56±0.23	0.34±0.14	0.33±0.13	0.30±0.12
Range	0.53-2.44	0.27-0.85	0.21-0.66	0.24-0.76	0.15-0.46	0.15-0.44	0.13-0.39
Dauer et al		0.44±0.38		0.42±0.36		0.17±0.15	0.11±0.11

Table 6 and 7 show that patient's body masses are greater in hospital B and also the number of images is higher which leads to higher KAP values and consequently to higher organ and tissue absorbed doses.

Following a method described earlier (Kramer et al 2008), CCs between risk of cancer incidence and mortality and the KAP have been calculated together with the organ absorbed doses in the Monte Carlo calculation using radiological risk coefficients from the BEIR VII report (NA/NRC, 2006). The results for the patients who underwent PA procedures are shown in tables 6 and 7.

Table 6. Anthropometric, dosimetric and risk-related data for the 12 PA patients in hospital A

Hospital A								
Gender	Age (y)	Mass (kg)	Height (cm)	Images Number	Fluoroscopy Time (min)	KAP ($Gy*cm^2$)	Cancer incidence Cases per 10^5 per KAP 10^{-5} $(Gy*cm^2)^{-1}$	Cancer mortality Cases per 10^5 per KAP 10^{-5} $(Gy*cm^2)^{-1}$
F	45	68	159	184	21.7	113.4	1.439	1.122
F	75	49	158	180	11.7	73.5	0.906	0.858
F	45	65	165	137	36	162.7	1.439	1.122
mean	55.0	60.7	160.7	167.0	23.1	116.5	1.261	1.034
M	70	49.7	156	218	11.2	131.4	0.760	0.695
M	64	66	171	323	47.1	193.9	0.896	0.788
M	70	81	168	354	31.2	731.1	0.576	0.533
M	72	53	160	176	25.8	139.0	0.696	0.649
M	35	81	169	362	14.3	235.8	0.841	0.663
M	65	53	165	139	12.3	187.1	0.862	0.759
M	72	49	162	128	14.2	65.4	0.696	0.649
M	63	73.7	166	176	12.6	186.7	0.765	0.665
M	62	69	163	206	26.9	319.8	0.783	0.676
mean	63.7	63.9	164.4	231.3	21.7	243.4	0.764	0.675

Table 7. Anthropometric, dosimetric and risk-related data for the 8 PA patients in hospital B

Hospital B								
Gender	Age (y)	Mass (kg)	Height (cm)	Images Number	Fluoroscopy Time (min)	KAP ($Gy*cm^2$)	Cancer incidence cases per 10^5 per KAP 10^{-5} $(Gy*cm^2)^{-1}$	Cancer mortality cases per 10^5 per KAP 10^{-5} $(Gy*cm^2)^{-1}$
F	58	68	162	317	10.4	462.7	1.840	1.527
F	67	60	160	147	11.1	169.7	1.797	1.595
F	85	100	160	390	17.5	755.2	0.703	0.698
F	83	69	152	198	29.4	587.8	0.816	0.810
mean	73.3	74.3	158.5	263.0	17.1	493.9	1.289	1.157
M	53	84	170	429	17.3	767.0	1.349	1.101
M	72	101	174	220	11.0	534.7	0.744	0.692
M	72	97	173	177	17.1	454.5	0.801	0.743
M	63	80	165	254	22.4	404.9	1.118	0.966
mean	65.00	90.50	170.50	270.00	16.9	540.3	1.003	0.876

Apart from the exposure conditions, especially the tube potential, and the patients mass and height, risk CCs depend on gender and age. Radiological cancer risks are higher for women than for men, mainly because of the increased breast cancer risk, and are higher for younger patients. With the data shown in tables 6 and 7 the absolute cancer risk can be calculated.

1. Example: First female patient in hospital B. The absolute risk for cancer mortality is $R = 1.527 * 10^{-5}\ (Gy*cm^2)^{-1} * 462.69\ (Gy*cm^2) = 7.07 * 10^{-3}$ or 0.71%

2. Example: Last male patient in hospital A. The absolute risk for cancer mortality is $R = 0.676 * 10^{-5}\ (Gy*cm^2)^{-1} * 319.82\ (Gy*cm^2) = 2.16 * 10^{-3}$ or 0.22%

Based on new epidemiological evidence, the ICRP emphasizes the optimization of exposures to specific tissues, particularly the lens of the eye, the heart and the cerebrovascular system (ICRP, 2012).

In this study, one patient was undergoing more than one procedure of hepatic chemoembolization. The accumulated absorbed dose to the heart for this patient was 498 mGy. This value is close to the absorbed dose threshold for circulatory disease (0.5 Gy) ICRP, 2012.

Insufficient collimation of the x-ray beam to the region of treatment is one of the possible causes of this fact. The majority of the procedures in this study were conducted by practitioners with few training in radiation protection. The figure 5 shows a) a case of non-appropriate collimation and b) a case of appropriate collimation during a hepatic arteriography in a chemoembolization procedure.

Figure 5. Image of a hepatic arteriography. (Left side) non-optimized collimation and (right side) proper collimation

4. CONCLUSIONS

In addition to reaching the thresholds for skin injuries to patients, other important organs can receive significant radiation doses in hepatic chemoembolization procedures compared with other diagnostic procedures.

The results show that apart from irradiation parameters, such as tube voltage, filtration, etc, organ and tissue absorbed doses depend aditionally on the patient´s body mass. Organ and tissue absorbed doses increase with the patient´s body mass.

In this work, organ and tissue conversion coefficients for the air kerma–area product for PA projection were calculated based on the anthropometric characteristics of the patients for a range of beam qualities used in hepatic chemoembolization interventional procedures that can serve to optimize radiological protection of patients submitted to this medical procedure.

5. REFERENCES

1. A. Trianni, D. Gasparini, and R. Padovani. Trigger levels to prevent reaction in interventional radiology procedures. *IFMBE Proceedings* **25**/III, pp. 410-413 (2009).

2. D. L. Miller, et al. Radiation doses in interventional radiology procedures: The RAD-IR Study, part II: Skin dose. *J Vasc Interv Radiol*. **14**, 977-990 (2003).

3. A. P. Cornetto, et al. Interventional radiology at a single institution over 9 years: A comprehensive evaluation of procedures and an estimation of collective effective dose. *J VascIntervRadiol*. **23**, 1665–1675 (2012).

4. International Commission on Radiation Units and measurements. *Patient Dosimetry for X Rays used in Medical Imaging*. ICRU Report 74. 5(2) (2005).

5. International Commission on Radiological Protection. *The 2007 recommendations of the International Commission on Radiological Protection*. ICRP Publication 103, Ann. ICRP 37 (2-4) (2007).

6. P. Johnson, et al. The influence of patient size on dose conversion coefficients: a hybrid phantom study for adult cardiac catheterization. *Phys. Med. Biol*. **54**, 3613–3629 (2009).

7. V. F. Cassola, et al. Standing adult human phantoms based on 10th, 50th and 90th mass and height percentiles of male and female Caucasian populations. *Phys. Med. Biol*. **56**, 3749–3772 (2011).

8. International Atomic Energy Agency. *Dosimetry in diagnostic radiology: an international code practice*. IAEA Technical reports series No 457, (2007).

9. V. F. Cassola, R. Kramer, C. Brayner and H. J. Khoury. Posture-specific phantoms representing female and male adults in Monte Carlo-based simulations for radiological protection. *Phys. Med. Biol*. **55**, 4399–4430 (2010).

10. www.caldose.org

11. Kawrakow I. and D.W.O. Rogers. *The EGSnrc code system: Monte Carlo simulation of electron and photon transport*, Report PIRS-701 (National Research Council of Canada, Ottawa), (2001).

12. Cranley K, Gilmore B. J, Fogarty G. W. A and Desponds L. IPEM Report 78: *Catalogue of diagnostic X-ray spectra and other data* (CD-Rom edition 1997) (electronic version prepared by D Sutton) (York: The Institute of Physics and Engineering in Medicine (IPEM) (1997).

13. R. Kramer, H. J. Khoury, and J. W. Vieira. CALDose_X-a software tool for the assessment of organ and tissue absorbed doses, effective dose and cancer risk in diagnostic radiology. *Phys. Med. Biol*. **53**(22), 6437-6459 (2008).

14. NA/NRC. National Academies/National Research Council. *Health Risks from Exposure to Low Levels of Ionizing Radiation*, BEIR VII, Phase 2 (National Academies Press, Washington) (2006).

15. International Comission on Radiological Protection. *Early and late effects of radiation in normal tissues and organs - Threshold Doses for Tissue Reactions in a Radiation Protection Context*. ICRP Publication 118. Ann. ICRP 41(1/2) (2012).

16. N. Hidajat, P. Wust, R. Felix, and R. J. Schröder. Radiation exposure to patient and staff in hepatic chemoembolization: Risk estimation of cancer and deterministic effects. *Cardiovasc Intervent Radiol* **29**, 791–796 (2006).

17. Dauer, L, T., Thornton, R., Boylan, D, C., Holahan, B., Prins, R., Quinn, B., and Germain, Jean St. Organ and effective dose estimates for patients undergoing hepatic arterial embolization for treatment of liver malignancy. *Med. Phys*. **38** (2), 736-742 (2011).